Electronic Supplementary Material (ESI) for Journal of Materials Chemistry A.

Supplementary information

Defect chemistry and transport properties of perovskite-type oxides $La_{1-x}Ca_xFeO_{3-\delta}$

Jia Song,[a] Shaochen Zhu,[a] De Ning[b] and Henny J.M. Bouwmeester*[acd]

[a]*Electrochemistry Research Group, Membrane Science and Technology, MESA+ Institute for Nanotechnology, University of Twente, P.O. Box 217, 7500 AE, Enschede, The Netherlands*

[b]*Helmholtz-Zentrum Berlin für Materialien und Energie, Hahn-Meitner-Platz 1, 14109 Berlin, Germany*

[c]*CAS Key Laboratory of Materials for Energy Conversion, Department of Materials Science and Engineering, University of Science and Technology of China, Hefei, 230026, P. R. China*

[d]*Forschungszentrum Jülich GmbH, Institute of Energy and Climate Research-IEK-1, Leo- Brandt-Str. 1, D-52425, Jülich, Germany*

Table S1 Structural data of $La_{1-x}Ca_xFeO_{3-\delta}$ from Rietveld refinements of room-temperature XRD data. The numbers in parentheses denote standard deviations in units of the least significant digits.

	Site	*x*	*y*	*z*	*B*	occ
***x* = 0.05**	*Pnma*, *a* = 5.54765(4) Å, *b* = 5.55665(3) Å, *c* = 7.84294(5) Å					
La	4c	0.9934(2)	0.02818(7)	0.25	0.67(1)	0.475
Ca	4c	0.9934(2)	0.02818(7)	0.25	0.67(1)	0.025
Fe	4b	0	0.5	0	0.47(1)	0.5
O1	8d	0.7178(11)	0.2798(11)	0.0340(9)	1.1(1)	1
O2	4c	0.0784(20)	0.4879(7)	0.25	2.5(2)	0.5
***x* = 0.10**	*Pnma*, *a* = 5.5408(1) Å, *b* = 5.54966(8) Å, *c* = 7.8318(1) Å					
La	4c	0.9940(5)	0.0268(1)	0.25	0.80(1)	0.45
Ca	4c	0.9940(5)	0.0268(1)	0.25	0.80(1)	0.05
Fe	4b	0	0.5	0	0.61(2)	0.5
O1	8d	0.7167(24)	0.2755(25)	0.0283(18)	0.8(2)	1
O2	4c	0.0948(40)	0.4896(18)	0.25	4.2(5)	0.5
***x* = 0.15**	*Pbnm*, a = 5.5298(1) Å, b = 5.54268(9) Å, c = 7.8163(1) Å					
La	4c	0.9938(6)	0.0256(1)	0.25	0.69(2)	0.4
Ca	4c	0.9938(6)	0.0256(1)	0.25	0.69(2)	0.1
Fe	4b	0	0.5	0	0.46(3)	0.5
O1	8d	0.7193(20)	0.2770(21)	0.0352(16)	0.4(2)	1
O2	4c	0.0794(39)	0.4898(14)	0.25	4.3(5)	0.5
***x* = 0.20**	*Pbnm*, *a* = 5.5216(1) Å, *b* = 5.5347(1) Å, *c* = 7.8045(1) Å					
La	4c	0.9948(8)	0.0240(1)	0.25	0.84(2)	0.4
Ca	4c	0.9948(8)	0.0240(1)	0.25	0.84(2)	0.1
Fe	4b	0	0.5	0	0.56(3)	0.5
O1	8d	0.7216(31)	0.2782(29)	0.0232(21)	0.2(2)	1
O2	4c	0.1092(37)	0.4927(21)	0.25	4.9(5)	0.5
***x* = 0.30**	*Pbnm*, *a* = 5.5026(1) Å, *b* = 5.52552(9) Å, *c* = 7.7778(1) Å					
La	4c	0.9950(5)	0.0216(1)	0.25	0.75(1)	0.35
Ca	4c	0.9950(5)	0.0216(1)	0.25	0.75(1)	0.15
Fe	4b	0	0.5	0	0.61(1)	0.5
O1	8d	0.7234(18)	0.2835(15)	0.0148(12)	0.15(9)	1
O2	4c	0.1179(20)	0.5012(14)	0.25	5.7(3)	0.5
***x* = 0.40**	*Pbnm*, *a* = 5.4882(1) Å, *b* = 5.5171(1) Å, *c* = 7.7572(1) Å					
La	4c	0.9991(12)	0.0215(1)	0.25	0.86(1)	0.3
Ca	4c	0.9991(12)	0.0215(1)	0.25	0.86(1)	0.2
Fe	4b	0	0.5	0	1.16(2)	0.5
O1	8d	0.7267(18)	0.2806(15)	0.0142(11)	0.09(9)	1
O2	4c	0.1391(18)	0.4939(17)	0.25	7.0(3)	0.5

Table S2 Activation energies of the chemical diffusion coefficient (D_{chem}) for $La_{1-x}Ca_xFeO_{3-\delta}$ derived from different temperature regions (designated by the space groups; *cf*. Fig. 3) in corresponding Arrhenius plots (Fig. 11a). Data are given for both oxidation (Ox) and reductions (Red) runs.

x	E_a (eV)			
	Red		Ox	
	Pbnm	$R\bar{3}c$	***Pbnm***	$R\bar{3}c$
0.05	1.80±0.02	-	1.80±0.02	-
0.10	1.46±0.02	1.05±0.07	1.45±0.02	1.04±0.07
0.15	1.40±0.02	0.97±0.04	1.42±0.03	0.96±0.04
0.20	1.12±0.01	0.75±0.01	1.17±0.01	0.75±0.01
0.30	1.53±0.01	0.98±0.01	1.40±0.04	0.95±0.01
0.40	-	1.09±0.02	-	1.02±0.02

Table S3 Activation energies of the oxygen self-diffusion coefficient (D_s) for $La_{1-x}Ca_xFeO_{3-\delta}$ derived from Arrhenius plots (Fig. 12a) along with the corresponding coefficients of determination (R^2) of the linear fitting. Data are given for both oxidation (Ox) and reductions (Red) runs.

x	Red		Ox	
	E_a (eV)	R^2 (-)	E_a (eV)	R^2 (-)
0.05	1.92±0.03	0.998	1.93±0.03	0.997
0.10	1.68±0.01	0.999	1.66±0.01	0.999
0.15	1.77±0.02	0.999	1.75±0.02	0.999
0.20	1.47±0.01	0.998	1.48±0.02	0.998
0.30	1.57±0.02	0.998	1.51±0.01	0.999
0.40	1.50±0.02	0.997	1.43±0.02	0.997

Table S4 Activation energies of the oxygen vacancy diffusion coefficient (D_v) for $La_{1-x}Ca_xFeO_{3-\delta}$ derived from Arrhenius plots (Fig. 12b) along with the corresponding coefficients of determination (R^2) of the linear fitting. Data are given for both oxidation (Ox) and reductions (Red) runs.

x	Red		Ox	
	ΔH_m **(eV)**	R^2 (-)	ΔH_m **(eV)**	R^2 (-)
0.05	1.72±0.02	0.998	1.72±0.03	0.997
0.10	1.44±0.02	0.998	1.43±0.02	0.998
0.15	1.41±0.02	0.998	1.39±0.02	0.998
0.20	1.18±0.03	0.994	1.20±0.03	0.993
0.30	1.17±0.02	0.997	1.15±0.02	0.997
0.40	1.11±0.03	0.994	1.05±0.03	0.992

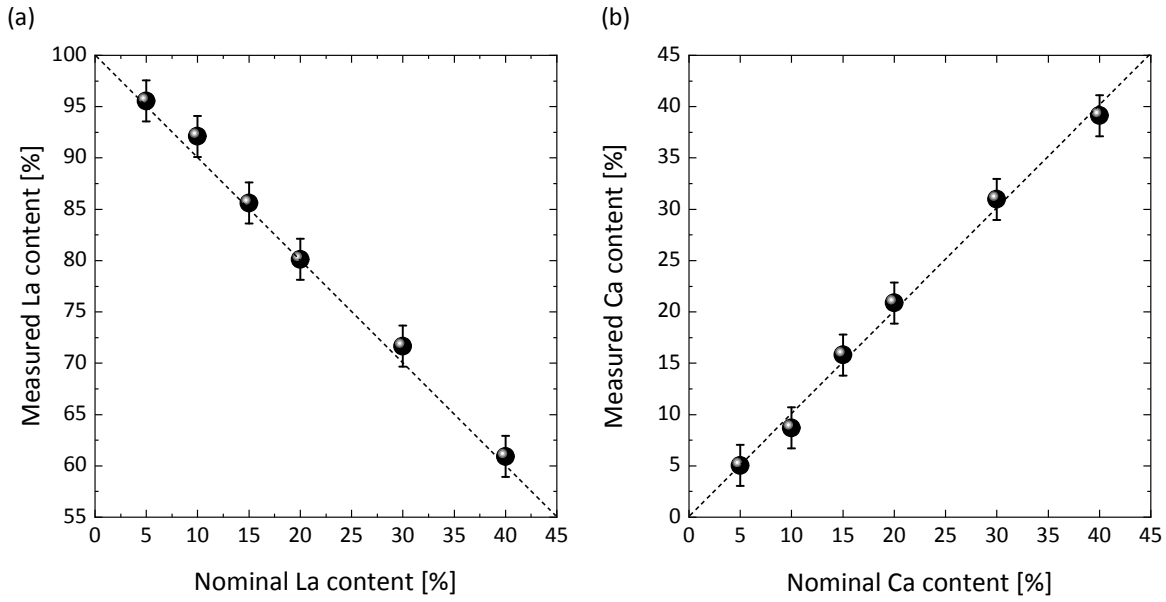

Fig. S1 Measured composition (by XRF analysis) vs nominal composition for samples $La_{1-x}Ca_xFeO_{3-\delta}$; (a) La content and (b) Ca content.

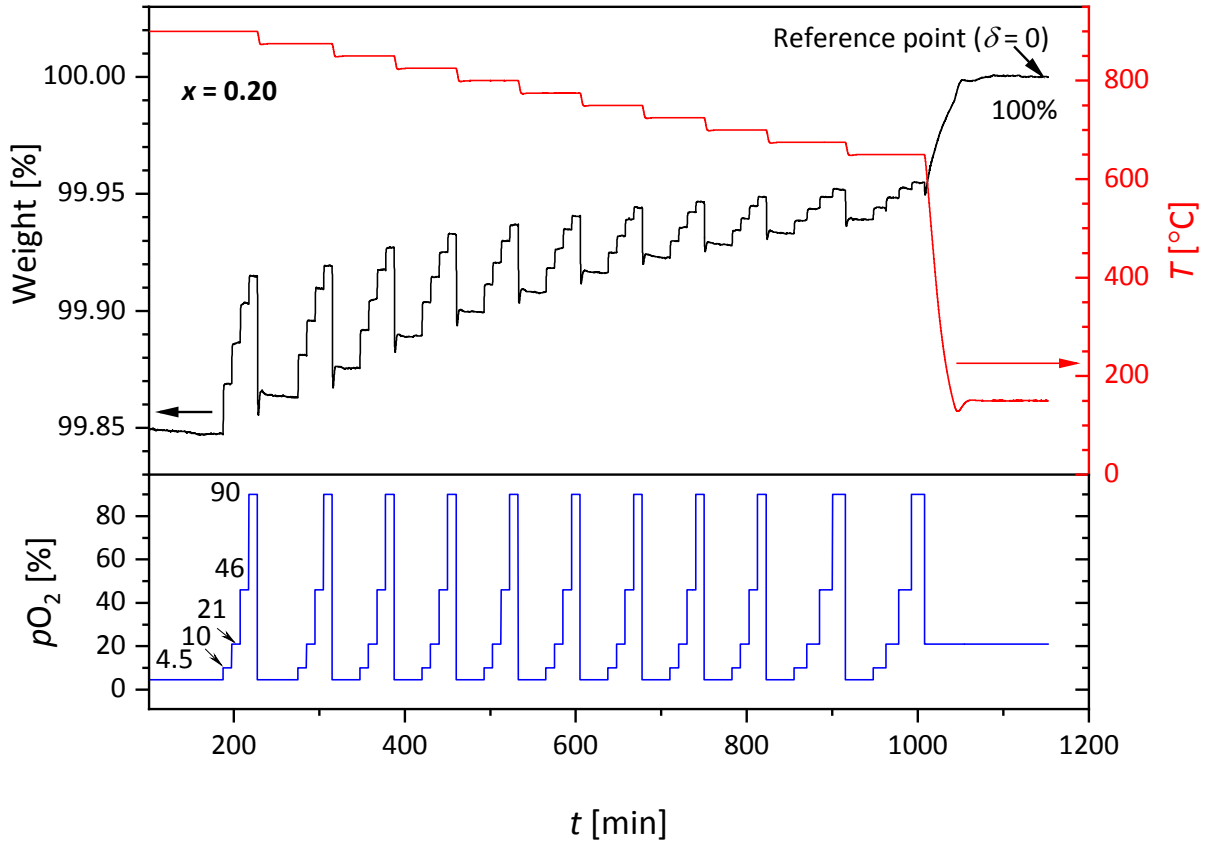

Fig. S2 Typical measurement scheme used for thermogravimetric analysis. Data shown are for $La_{1-x}Ca_xFeO_{3-\delta}$ (x = 0.20).

(a)

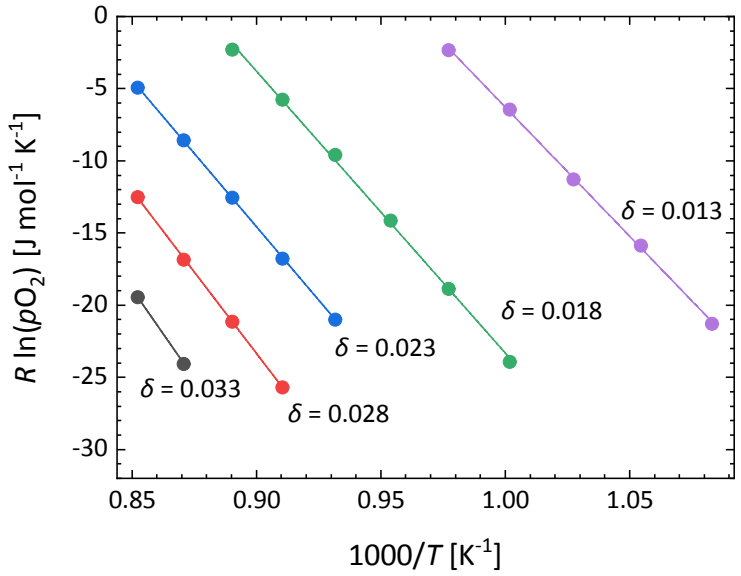
0
-5
-10
-15
-20
-25
-30
0.85
0.90
0.95
1.00
1.05
$R \ln(pO_2)$ [J mol^{-1} K^{-1}]
1000/T [K^{-1}]
δ = 0.013
δ = 0.018
δ = 0.023
δ = 0.028
δ = 0.033

(b)

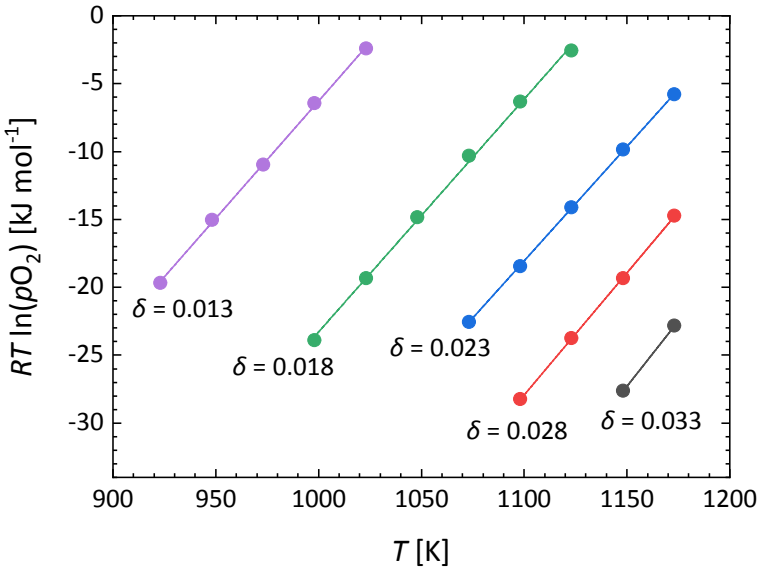
0
-5
-10
-15
-20
-25
-30
900
950
1000
1050
1100
1150
1200
$RT \ln(pO_2)$ [kJ mol^{-1}]
T [K]
δ = 0.013
δ = 0.018
δ = 0.023
δ = 0.028
δ = 0.033

(c)

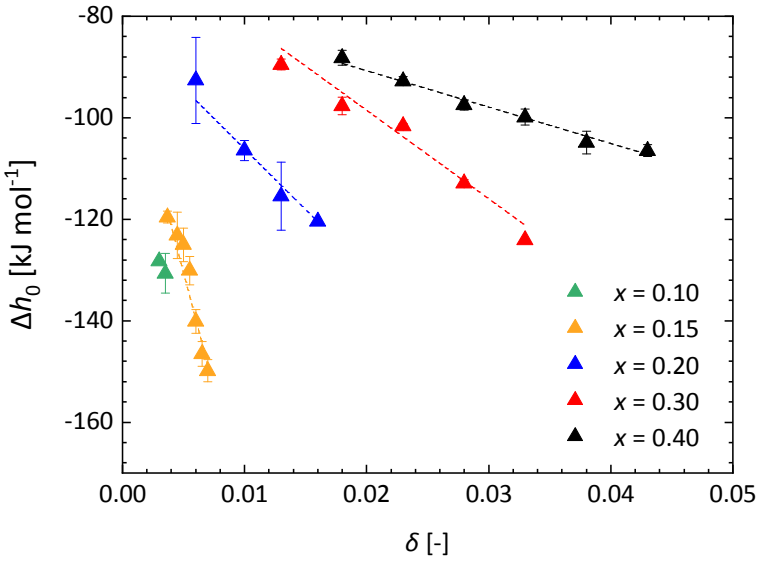

(d)

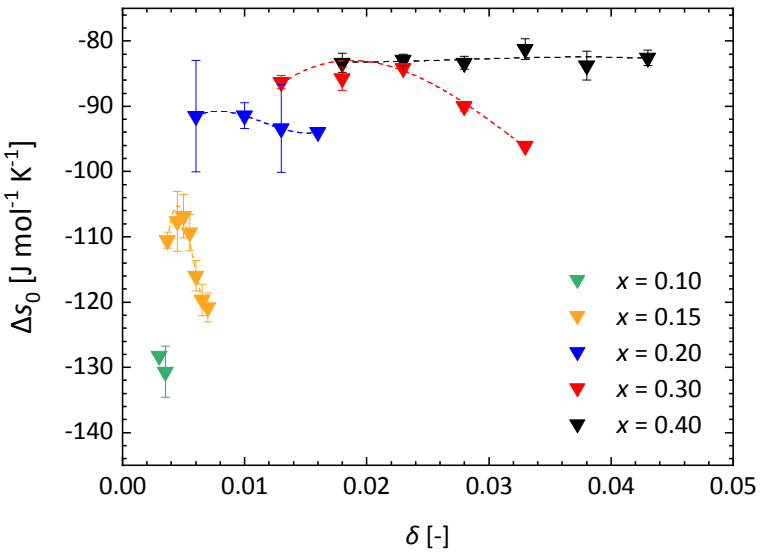

Fig. S3 (a) $^{R\ln(pO_2)}$ vs $1/T$ and (b) $^{RT\ln(pO_2)}$ vs T plots for $La_{0.7}Ca_{0.3}FeO_{3-\delta}$, at given values of δ, used for evaluation of the partial molar enthalpy of oxygen, $^{\Delta h_O}$, and the partial molar entropy of oxygen, $^{\Delta s_O}$. (c) $^{\Delta h_O}$ and (d) $^{\Delta s_O}$, at given values of x in $La_{1-x}Ca_xFeO_{3-\delta}$, as a function of δ as derived from similar $^{R\ln(pO_2)}$ vs $1/T$ and $^{RT\ln(pO_2)}$ vs T plots.

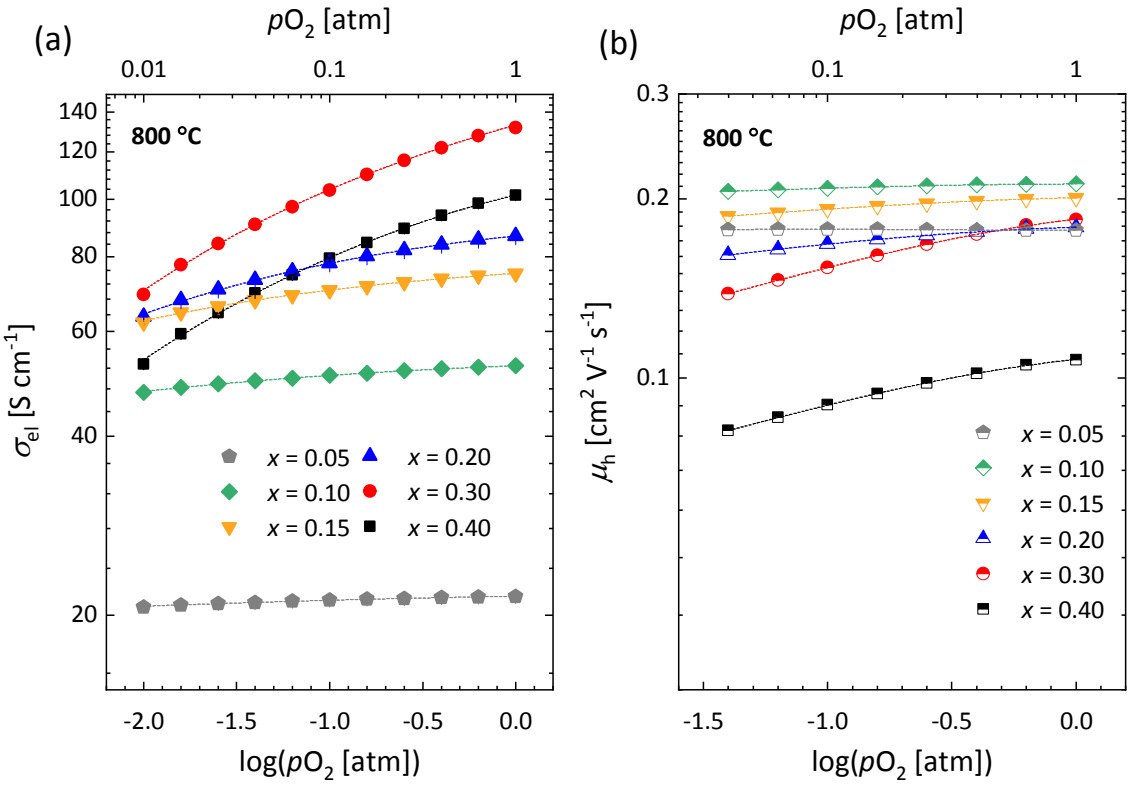

Fig. S4 pO_2 dependence of the (a) electrical conductivity (σ_{el}) and (b) electrical mobility (μ_h) for $La_{1-x}Ca_xFeO_{3-\delta}$ at 800 °C. The dashed lines are drawn to guide the eye.

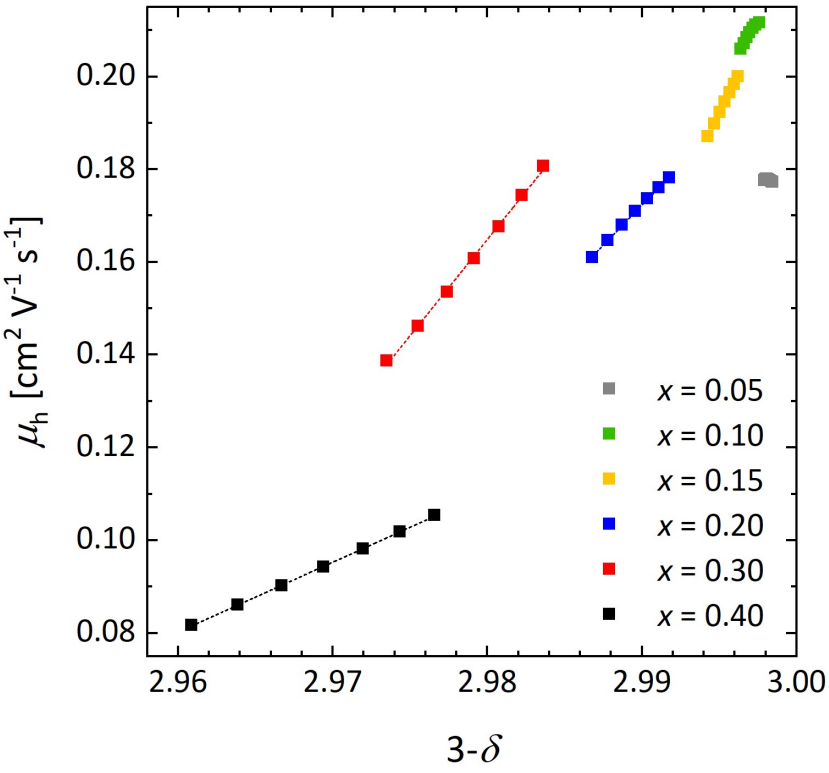

Fig. S5 Mobility of electron holes (μ_h), at 800 °C, for $La_{1-x}Ca_xFeO_{3-\delta}$ as a function of oxygen content ($3-\delta$). The dashed lines are drawn to guide the eye.

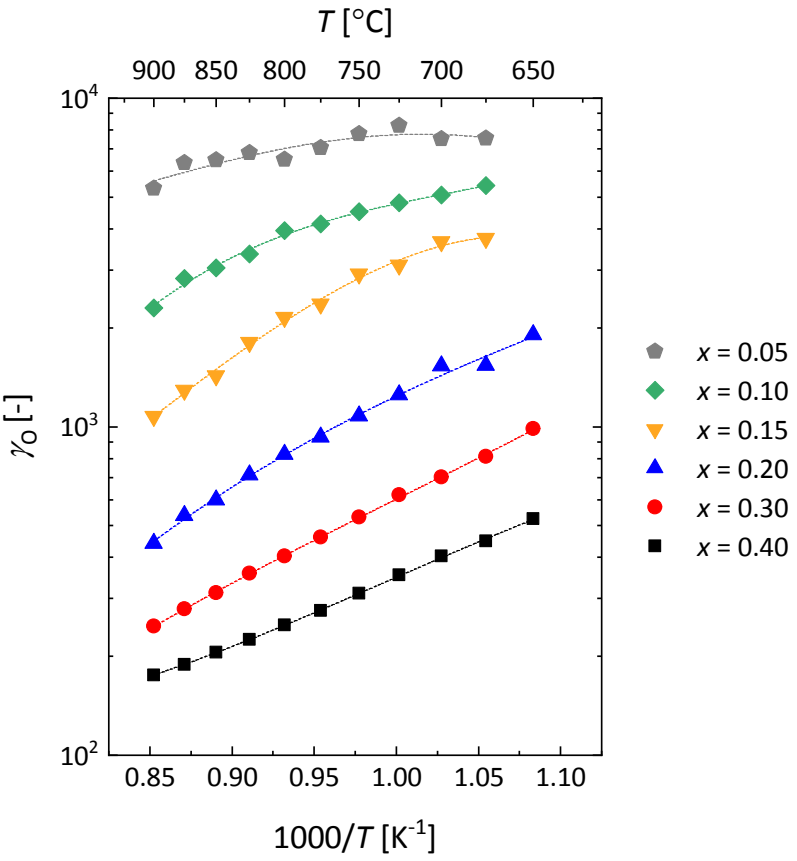

Fig. S6 Inverse temperature dependence of the thermodynamic factor for $La_{1-x}Ca_xFeO_{3-\delta}$, at pO_2 = 0.147 atm, calculated from data of thermogravimetry (*cf*. Fig. 4). The specified pO_2 corresponds to the logarithmic average of the step change in pO_2 (0.10 ↔ 0.215 atm) used in the ECR measurements.

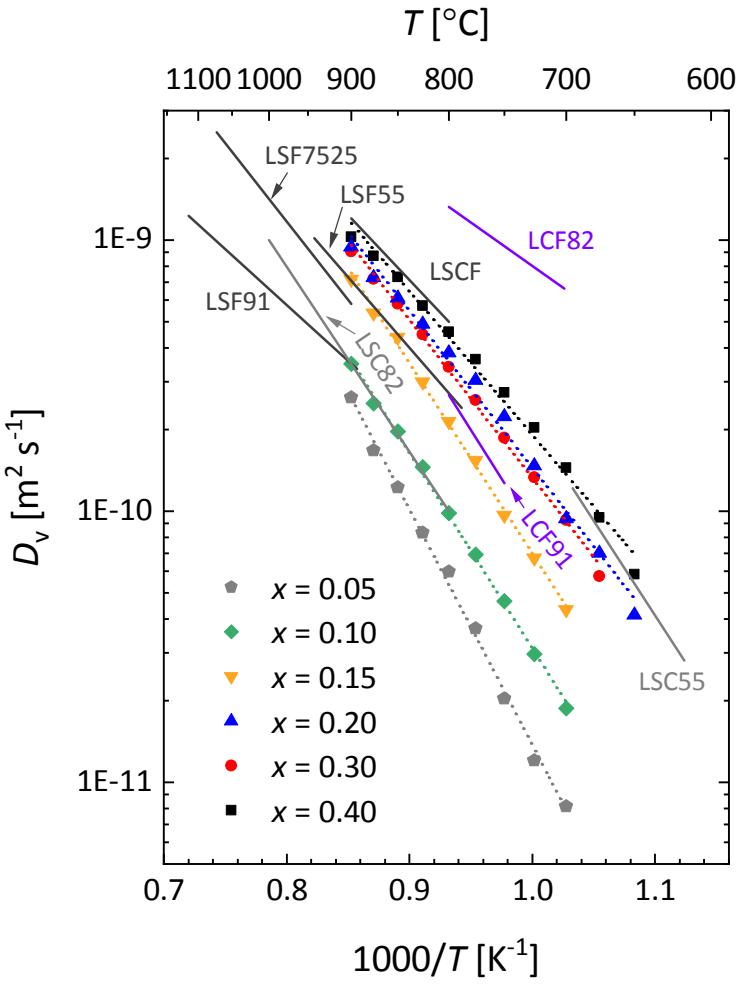

Fig. S7 Comparison of the oxygen vacancy diffusion coefficients (D_V) for $La_{1-x}Ca_xFeO_{3-\delta}$ (this work) with data for selected perovskite-type oxides from literature. Data for $La_{0.9}Ca_{0.1}FeO_{3-\delta}$ (LCF91) from Ref. 1, $La_{0.8}Ca_{0.2}FeO_{3-\delta}$ (LCF92) from Ref. 2, $La_{1-x}Sr_xFeO_{3-\delta}$ (x = 0.1 (LSF91), x = 0.25 (LSF7525)) from Ref. 3, $La_{0.5}Sr_{0.5}FeO_{3-\delta}$ (LSF55) from Ref. 4, $La_{1-x}Sr_xCoO_{3-\delta}$ (x = 0.2 (LSC82), x = 0.5 (LSF55)) from Ref. 5, and $La_{0.6}Sr_{0.4}Co_{0.2}Fe_{0.8}O_{3-\delta}$ (LSCF) from Ref. 6.

References

1 C. Berger, E. Bucher, and W. Sitte, Solid State Ionics, 2017, **299**, 46-54.
2 C. Berger, E. Bucher, A. Windischbache, A. D. Boese, and W. Sitte, 2018, **259**, 57-66.
3 T. Ishigaki, S. Yamauchi, K. Kishio, J. Mizusaki and K. Fueki, J. Solid State Chem., 1988, **73**, 179–187.
4 J. Yoo, A. Verma, S. Y. Wang, and A. J. Jacobson, J. Electrochem. Soc., 2005, **152**, A497
5 R. A. De Souza, and J. A. Kilner, 1998, **106**, 175-187.
6 A. Esquirol, J. A. Kilner, and N. Brandon, 2004, **175**, 63-67.